A Methodology for Optimal Distributed Storage Planning in Smart Distribution Grids

Mohammad Ghasemi Damavandi, *Student Member, IEEE*, José R. Martí, *Life Fellow, IEEE*, and Vikram Krishnamurthy, *Fellow, IEEE*

***Abstract*—This paper proposes a methodology for optimal planning of distributed storage systems (DSS) in smart grids with high penetration of renewable sources. The DSS can provide distribution systems with various benefits, including arbitrage gain, reduction in the system losses, system resilience enhancement, reduction in nondispatchable energy curtailment, and peak load shaving. In particular, by alleviating the peak load, the system upgrade time can be deferred to future years, resulting in noticeable financial gains for the system operator. In this paper, the problem of DSS planning for optimizing the discounted economic gain of the system operator is formulated and solved as a mixed-integer convex program. Various economic gains are taken into account and the stochasticity of the loads and renewable generations is accounted for by evaluating the total expected gain. Numerical results for DSS planning on a 69-node, 11-kV smart grid and using real data of smart meters and renewable energy sources are presented and discussed.**

***Index Terms*—Distributed generators (DG), distributed storage systems (DSS), renewable energy, smart grids (SG).**

I. Introduction

SMART distribution systems can benefit from high penetration of renewable energy sources distributed in the grid. Parts of the future distribution systems are even envisioned to work as microgrids where during the islanded mode the demand power should be completely supplied by local Distributed Generators (DGs). These DGs are often highly intermittent and can cause dramatic changes in the demand/generation of the nodes.

When the amount of non-dispatchable renewable energy generation is forecast to violate a technical or contractual system constraint, the Smart Grid Operator (SGO) will have to curtail the excess power or store it in Distributed Storage Systems (DSS). Therefore, using DSS the SGO will be able to gain some profit by storing the excess energy that would be spilled otherwise. Furthermore, in virtue of DSS, the SGO will be able store energy at off-peak hours and sell it at peak hours when the demand is higher. In markets with Time of Use (ToU) energy pricing [1], that naturally translates into an arbitrage gain for the SGO. The power losses in the system will also decrease by shaving the load at peak hours. If the system undergoes a fault, the SGO will also have the degree of freedom to take advantage of these DSS during the system restoration time to minimize the energy-not-supplied [2]. In other words, the resilience of the system is improved by means of DSS. Moreover, the SGO can employ the DSS for peak load shaping [3] and thereby defer the upgrade of the system which will be inevitable due to constant load growth in distribution systems [4]. If the budget required for the system upgrade is noticeable, the deferral of the system upgrade may result in considerable financial gains due to interest rates. Other advantages of the DSS include voltage control [5], [6], ancillary services, and power smoothing for solar arrays [7]. As a result, several authors have considered the use of DSS for distribution systems with high penetration of wind and photovoltaic generation [8], [9].

The optimal DSS planning has been considered in several recent works [10]–[19]. In [10], a framework is presented which optimizes the capacity and power rating of DSS to ensure that the renewable energy generated by DGs never spill. Nonetheless, this work does not consider various other advantages that the DDS introduce to the system. In [11], the potential of DSS in the low-voltage distribution grid for deferring upgrades needed to increase the solar penetration level is investigated. In [12], the optimal allocation of DSS in distribution systems using a multi-objective optimization approach is considered. However, [11] and [12] do not consider the role of DSS in improving the resilience of the system. In [13], a methodology for DSS allocation in distribution systems is proposed which aims at cost-effective improvement of the system reliability. In [14], the optimal planning of DSS using the point estimate method is considered. In [15] and [16], the optimal placement of DSS considering the benefits due to system upgrade deferral is investigated using genetic algorithm. Genetic algorithm is also used in [17] for DSS planning in smart grids. In [18] and [19], DSS planning methodologies are proposed where the stochasticity of the loads and renewable energy sources is treated using scenario based approaches.

This paper proposes a new methodology for optimal DSS planning in smart distribution systems using linearized power

Manuscript received October 4, 2016; revised February 2, 2017, May 14, 2017, and August 19, 2017; accepted October 2, 2017. Date of publication October 6, 2017; date of current version March 20, 2018. This work was supported in part by the National Science Foundation under Grant 1714180, and in part by the Schmidt Sciences. Paper number TSTE-00757-2016. *(Corresponding author: Mohammad Ghasemi Damavandi.)*

M. G. Damavandi and J. R. Martí are with the Department of Electrical and Computer Engineering, University of British Columbia, Vancouver, BC V6T 1Z4, Canada (e-mail: mghasemi@ece.ubc.ca; jrms@ece.ubc.ca).

V. Krishnamurthy is with the School of Electrical and Computer Engineering, and the Cornell Tech, Cornell University, New York, NY 10044 USA (e-mail: vikramk@cornell.edu).

Color versions of one or more of the figures in this paper are available online at http://ieeexplore.ieee.org.

Digital Object Identifier 10.1109/TSTE.2017.2759733

flow equations [20]. In particular, the aim of this paper is to present a novel formulation that is *simultaneously*:

1) Comprehensive, in that all the economic gains due to installation of DSS are incorporated.
2) Statistically rigorous, in that the stochasticity of the loads and renewable energy sources is treated by explicitly evaluating the mathematical expectations.
3) Tractable, in that the problem is formulated as a mixed-integer convex[1] program.

The methodology proposed in the present paper jointly optimizes the number of storage units to be installed, their location, their power rating and capacity, and their optimal active/reactive strategy of charging and discharging. The financial gains due to price arbitrage, reduction in the system losses, reduction in the renewable energy curtailed, system resilience enhancement, and system upgrade deferral are formulated in the presented methodology. The stochasticity of the loads and renewable energy sources is accounted for by evaluating the expected discounted gains using the Law of Large Numbers (LLN). In addition, the optimal planning problem is formulated as a mixed-integer convex program to be solved using branch and bound algorithms. The proposed methodology has been tested on a typical distribution system using real data of smart meters and renewable energy sources and the results are presented and discussed.

The rest of the paper is organized as follows. Section II provides some preliminaries about the linearized power flow equations in distribution systems. Section III formulates various financial gains due to installation of DSS in distribution systems. Section IV presents a mixed-integer convex formulation of the problem of distributed storage planning in smart distribution systems. Section V provides the numerical results of the optimal DSS placement in a test system. Finally, Section VI concludes the paper.

II. Linearized Power Flow Equations in Rectangular Coordinates

This section reviews the linearized power flow equations in rectangular coordinates for application in distribution systems [20]–[22]. The section also provides some numerical results to demonstrate the effectiveness of these equations in distribution systems with DGs. Throughout the paper, constant active and reactive power consumption is assumed for the nodes.

Consider a distribution system with N nodes and let the voltage of the nth node be represented in rectangular coordinates as $v_n = 1 + \tilde{v}_n = 1 + \mathrm{e}_n + j\mathrm{f}_n$. Without loss of generality, assume that the first node is the slack node with a given voltage of 1 p.u. Let $\tilde{v} = [\tilde{v}_2, \tilde{v}_3, \ldots, \tilde{v}_N]^T$ denote the vector of deviations from the flat voltage profile at the remaining nodes of the system. Also, let $\mathrm{e} = [\mathrm{e}_2, \mathrm{e}_3, \ldots, \mathrm{e}_N]^T$ and $\mathrm{f} = [\mathrm{f}_2, \mathrm{f}_3, \ldots, \mathrm{f}_N]^T$ represent the real and imaginary parts of $\tilde{v}$. These vectors can be approximated by linearized power flow equations in rectangular coordinates provided that their elements are small [21]. For real distribution systems it is a known fact that the elements of f are very small (i.e., the voltage angles with respect to the slack node are very small.) The operational constraints of distribution systems also require that the elements of e remain small (e.g., within ± 0.06 p.u.) at peak hours.[2] At off-peak hours, the elements of e are even smaller which make the linearized power flow equations more accurate [23].

Let $\mathbf{Y}_{N\times N} = \mathbf{G} + j\mathbf{B}$ be the bus admittance matrix of the system where $\mathbf{G}$ and $\mathbf{B}$ are the bus conductance and bus susceptance matrices, respectively. By removing the first row and column of $\mathbf{Y}$, an $(N-1)\times(N-1)$ submatrix corresponding to the non-slack nodes is obtained which we denote by $\tilde{\mathbf{Y}} = \tilde{\mathbf{G}} + j\tilde{\mathbf{B}}$. Using these matrices and assuming that no shunt capacitor is installed in the system, the linearized power flow equations can be written as [21]:

$$\begin{bmatrix} \mathrm{p} \\ \mathrm{q} \end{bmatrix} - \begin{bmatrix} \mathrm{p}_{\mathrm{DG}} \\ \mathrm{q}_{\mathrm{DG}} \end{bmatrix} = \mathbf{A}^{-1} \begin{bmatrix} \mathrm{e} \\ \mathrm{f} \end{bmatrix} \tag{1}$$

where $\mathrm{p} = [p_2, p_3, \ldots, p_N]^T$ and $\mathrm{q} = [q_2, q_3, \ldots, q_N]^T$ are the vector of active and reactive power consumptions of the nodes, respectively. Similarly, $\mathrm{p}_{\mathrm{DG}} = [p_{\mathrm{DG},2}, p_{\mathrm{DG},3}, \ldots, p_{\mathrm{DG},N}]^T$ and $\mathrm{q}_{\mathrm{DG}} = [q_{\mathrm{DG},2}, q_{\mathrm{DG},3}, \ldots, q_{\mathrm{DG},N}]^T$ are the vector of active and reactive power generation by local DGs, respectively. Moreover, $\mathbf{A}$ is defined as:

$$\mathbf{A} = \begin{bmatrix} \tilde{\mathbf{G}} & -\tilde{\mathbf{B}} \\ -\tilde{\mathbf{B}} & -\tilde{\mathbf{G}} \end{bmatrix}^{-1}. \tag{2}$$

Rearranging the matrix form of the linearized power flow equations, (1) reads as:

$$\begin{aligned} (\mathrm{p} - j\mathrm{q}) - (\mathrm{p}_{\mathrm{DG}} - j\mathrm{q}_{\mathrm{DG}}) &= (\tilde{\mathbf{G}}\mathrm{g} - \tilde{\mathbf{B}}\mathrm{f}) + j(\tilde{\mathbf{B}}\mathrm{g} + \tilde{\mathbf{G}}\mathrm{f}) \\ &= (\tilde{\mathbf{G}} + j\tilde{\mathbf{B}})(\mathrm{g} + j\mathrm{f}), \end{aligned} \tag{3}$$

or, equivalently,

$$\mathrm{s}^* - \mathrm{s}^*_{\mathrm{DG}} = \tilde{\mathbf{Y}}\tilde{v}, \tag{4}$$

where $\mathrm{s} = \mathrm{p} + j\mathrm{q}$ is the vector of complex power consumption of the nodes, $\mathrm{s}_{\mathrm{DG}} = \mathrm{p}_{\mathrm{DG}} + j\mathrm{q}_{\mathrm{DG}}$ is the vector of complex power injections by local DGs, and $(\cdot)^*$ denotes complex conjugation. Equation (4) is the complex form derived in [20] with appropriate modifications to account for DGs. In [20], the authors have presented the mathematical and practical conditions under which the linearized power flow equations provide valid solutions. They have also used the complex form of (4) to theoretically bound the approximation error of the linearized equations. The interested reader is referred to to [20] for full mathematical analysis of the linearized power flow equations.

Using linearized power flow equations, the active power loss in the system can also be approximated as a quadratic function of power injections. To see this, define the *net demand vector* d as:

$$\mathrm{d} = \begin{bmatrix} \mathrm{p} \\ \mathrm{q} \end{bmatrix} - \begin{bmatrix} \mathrm{p}_{\mathrm{DG}} \\ \mathrm{q}_{\mathrm{DG}} \end{bmatrix} \tag{5}$$

[1] With slight abuse of terminology, the term mixed-integer convex programming is used in this paper to refer to the problems that are non-convex merely due to the integrality of some variables. Therefore, these problems become convex if the integrality constraints are relaxed.

[2] Although the operational constraints are usually imposed on the magnitude of the nodal voltages, the voltage magnitudes in distribution systems are very well approximated by their real parts.

Based on (5), the linearized equations can be written in the following compact form:

$$\begin{bmatrix} \mathbf{e} \\ \mathbf{f} \end{bmatrix} = \mathbf{A}\mathbf{d}. \tag{6}$$

Using (6), it is shown in the Appendix A that the total active power loss in the system can be written in terms of the net demand vector as:

$$L(\mathbf{d}) = \frac{1}{2}\mathbf{d}^T\mathbf{M}\mathbf{d}, \tag{7}$$

where

$$\mathbf{M} = 2\mathbf{A}^T \begin{bmatrix} \tilde{\mathbf{G}} & \mathbf{0} \\ \mathbf{0} & \tilde{\mathbf{G}} \end{bmatrix} \mathbf{A}, \tag{8}$$

is a $2(N-1) \times 2(N-1)$ symmetric real matrix that depends merely on the bus conductance and bus susceptance matrices of the system. Using (7) and (8), it is also shown in Appendix A that the loss function is convex in $\mathbf{d}$.

To illustrate the effectiveness of the linearized power flow equations, we consider a modified version of the 69-node, 11 kV distribution system presented in [24]. For this system, inclined solar cells are considered on half of the nodes selected randomly. Moreover, two wind turbines are installed on the nodes 21 and 50 with power ratings of 400 kW and 800 kW, respectively. Real data of the loads, wind and solar generations are exploited for this illustration. Details about the test system and the real data used will be provided in Section V. All the numbers reported here are obtained by simulating the system for 535 days, 24 hours each. For each simulation, the error of the linearized power flow equations is computed in comparison with the Newton's AC Power Flow (ACPF) in terms of Average Magnitude Error (AME) in p.u., Average Angle Error (AAE) in degrees, Maximum Magnitude Error (MME) in p.u., Maximum Angle Error (MAE) in degrees, and Normalized Loss Error (NLE). In particular, these metrics are defined as follows:

$$\begin{aligned}
\text{AME} &= \frac{1}{N}\sum_{n=1}^{N}\Big||v_{n,\text{lin}}| - |v_{n,\text{ACPF}}|\Big| \\
\text{AAE} &= \frac{1}{N}\sum_{n=1}^{N}\Big|\angle v_{n,\text{lin}} - \angle v_{n,\text{ACPF}}\Big| \\
\text{MME} &= \max_n \Big||v_{n,\text{lin}}| - |v_{n,\text{ACPF}}|\Big| \\
\text{MAE} &= \max_n \Big|\angle v_{n,\text{lin}} - \angle v_{n,\text{ACPF}}\Big| \\
\text{NLE} &= \frac{\Big|L_{\text{lin}} - L_{\text{ACPF}}\Big|}{L_{\text{ACPF}}},
\end{aligned} \tag{9}$$

where the subscript *lin* indicates the solution of the linearized power flow equations. For the test system under study and using the real data of loads, wind, and solar generation, the AME and AAE indexes averaged over all simulations are 3.84×10^{-4} p.u. and 1.04×10^{-3} degrees, respectively. Also, the MME and MAE indexes averaged over all simulations turn out to be 1.45×10^{-3} p.u. and 9.31×10^{-3} degrees, respectively. Moreover, the NLE averaged over all simulations turns out to be 3.05%. These numbers show that the linearized power flow equations can provide good approximations in terms of nodal voltages and system power losses.

III. Formulation of the Economic Gains of the Distributed Storage Systems

This section formulates the various economic gains of the DSS for smart distribution grids. Due to the stochasticity of the loads, wind and solar generations, the expected economic gain of the SGO due to installation of storage units is considered. To ensure a longer lifetime for the DSS, similarly to [10], [25], it is assumed that the storage units are charged and discharged once a day. In particular, for each day, there is one charging cycle corresponding to off-peak hours and one discharging cycle corresponding to peak hours. This cycling strategy is also considered fixed during the planning horizon. Once the storage units are optimally planned for the system, their daily charging and discharging periods can be further optimized based on the day-to-day profile of the loads and renewable energy sources. This idea is explored in [1], where the contributions of [10] and [25] are extended to include flexible charging/discharging periods for daily operation of the storage units.

The proposed methodology in this paper seeks an optimal DSS planning which optimizes the number of storage units, their location, their power rating and capacity, and their optimal charging and discharging strategy jointly. In addition, the proposed methodology presents a framework in which the stochasticity of the real data of loads and renewable energy sources is taken into account. Analysis of the real data of smart meters, wind turbines, and solar cells demonstrates that the load and renewable energy sources have hourly and seasonal patterns. As a result, the optimal charging and discharging strategy of the DSS will inevitably be different for different hours of the day and different segments of the year. Therefore, the proposed methodology allows for different charging and discharging strategies for different hours of the day and different segments of the year. To that end, the planning horizon consists of Y years and each year is divided into S segments. For hour h of segment s, let $\mathbf{p}_{s,h}^{\text{DSS}}$ be the vector of charging/discharging active powers by the storage units installed in the system. Similarly, let $\mathbf{q}_{s,h}^{\text{DSS}}$ be the vector of charging/discharging reactive powers by the storage units at hour h of segment s. If the result of the optimal planning does not assign a storage unit to a node, the corresponding active and reactive powers will equivalently remain zero at all time. Thus, the number of storage units is optimized. To simplify the notation, define $\mathbf{d}_{s,h}^{\text{DSS}} = \left[[\mathbf{p}_{s,h}^{\text{DSS}}]^T, [\mathbf{q}_{s,h}^{\text{DSS}}]^T\right]^T$ for the storage units at hour h of segment s. In general, the charging/discharging strategy of each storage unit can be optimized not only for each hour and each segment, but also for each year. However, we restrict ourselves to the case where the optimized strategy for each hour and segment remains the same for all years. That is because even though the load and renewable generations grow over years, the capacity of the DSS remains fixed for the whole planning horizon. Nonetheless, the proposed methodology can simply accommodate the case where

the DSS strategy is optimized for each year, in addition to optimizing for each hour and each segment. We will denote the operation strategy of the DSS in the sth segment of each year by $\pi_s = \left[[\mathbf{d}^{\text{DSS}}_{s,1}]^T, [\mathbf{d}^{\text{DSS}}_{s,2}]^T, \cdots, [\mathbf{d}^{\text{DSS}}_{s,24}]^T\right]^T$. Also, the matrix of DSS operation strategies for the whole planning horizon will be denoted by $\mathbf{\Pi} = [\pi_1, \pi_2, \ldots, \pi_{\mathsf{S}}]$.

A. The Arbitrage Gain

To evaluate the arbitrage gain of the SGO due to installation of DSS, a Time of Use (ToU) pricing scheme is considered in this paper. Let $\eta^y_{s,h}$ be the price of electricity per kWh at hour h of the sth segment of the yth year of the planning horizon. The average arbitrage gain in the yth year can be written as:

$$\Gamma^{\text{arb}}_y(\mathbf{\Pi}) = \frac{365}{\mathsf{S}} \sum_{s=1}^{\mathsf{S}} \left\{ \sum_{h\in\mathcal{H}_p} \eta^y_{s,h} \mathbf{1}^T \mathbf{p}^{\text{DSS}}_{s,h} - \sum_{h\in\mathcal{H}_o} \eta^y_{s,h} \mathbf{1}^T \mathbf{p}^{\text{DSS}}_{s,h} \right\}, \tag{10}$$

where $\mathcal{H}_p$ is the set of candidate discharging hours (peak hours) and $\mathcal{H}_o = \{1, 2, \ldots, 24\} \setminus \mathcal{H}_p$ is the set of candidate charging hours (off-peak hours). Observe from (10) that the average arbitrage gain of the SGO is linear in $\mathbf{\Pi}$.

B. The Expected Reduction in Active Power Loss

In this section, the expected economic gain of the SGO due to reduction in the active power loss is formulated. The expected daily power loss of the system in the sth segment of the yth year as a funciton of the DSS operation strategy can be written as:

$$\mathbb{E}\left\{\sum_{h=1}^{24} \mathrm{L}^y_{s,h}\left(\mathbf{d}^{\text{DSS}}_{s,h}\right)\right\} = \sum_{h\in\mathcal{H}_o} \mathbb{E}\left\{L\left(\mathbf{d}^y_{s,h} + \mathbf{d}^{\text{DSS}}_{s,h}\right)\right\} + \sum_{h\in\mathcal{H}_p} \mathbb{E}\left\{L\left(\mathbf{d}^y_{s,h} - \mathbf{d}^{\text{DSS}}_{s,h}\right)\right\}, \tag{11}$$

where the $L(\cdot)$ function is defined in (7) and $\mathbb{E}\{\cdot\}$ denotes the expectation operator. Here, $\mathbf{d}^y_{s,h} = \left[[\mathbf{p}^y_{s,h}]^T, [\mathbf{q}^y_{s,h}]^T\right]^T$ is the vector of stochastic net demands at hour h of the sth segment of the yth year. Expanding (11) using (7) and considering the ToU pricing scheme, the expected daily cost due to the active power loss in the sth segment of the yth year can be written as:

$$\begin{aligned}\mathbb{E}\left\{\sum_{h=1}^{24} \eta^y_{s,h}\mathrm{L}^y_{s,h}\left(\mathbf{d}^{\text{DSS}}_{s,h}\right)\right\} &= \frac{1}{2}\sum_{h=1}^{24} \eta^y_{s,h}\left[\mathbf{d}^{\text{DSS}}_{s,h}\right]^T \mathbf{M}\left[\mathbf{d}^{\text{DSS}}_{s,h}\right] \\ &+ \sum_{h\in\mathcal{H}_o} \eta^y_{s,h}[\bar{\mathbf{d}}^y_{s,h}]^T \mathbf{M}\, \mathbf{d}^{\text{DSS}}_{s,h} \\ &- \sum_{h\in\mathcal{H}_p} \eta^y_{s,h}[\bar{\mathbf{d}}^y_{s,h}]^T \mathbf{M}\, \mathbf{d}^{\text{DSS}}_{s,h} \\ &+ \sum_{h=1}^{24} \eta^y_{s,h} c^y_{s,h}, \end{aligned} \tag{12}$$

where $\bar{\mathbf{d}}^y_{s,h} = \mathbb{E}\left\{\mathbf{d}^y_{s,h}\right\}$, and

$$c^y_{s,h} = \mathbb{E}\left\{\mathrm{L}^y_{s,h}(\mathbf{0})\right\} = \frac{1}{2}\mathbb{E}\left\{[\mathbf{d}^y_{s,h}]^T\, \mathbf{M}\, [\mathbf{d}^y_{s,h}]\right\}, \tag{13}$$

is the expected hourly power loss in the sth segment of the yth year when no DSS is installed in the system.

Leveraging the Law of Large Numbers (LLN), it is possible to use the real data of the loads and renewable generations to approximate $\bar{\mathbf{d}}^y_{s,h}$ with the empirical mean which is an unbiased estimator. Let $d^0_{s,h}(l)$ be the lth random element of the net demand vector $\mathbf{d}^0_{s,h}$ at the first year. Also, assume that at the planning time a total number of K_s real data points of the load and renewable generation is available for each hour of segment s. With slight abuse of notation, let $d^0_{s,h}(l,k)$ be the kth measured data corresponding to the lth element of the net demand vector at hour h and segment s. Then, based on LLN, $\bar{d}^0_{s,h}(l)$ can be approximated as:

$$\bar{d}^0_{s,h}(l) = \mathbb{E}\{d^0_{s,h}(l)\} \approx \frac{1}{K_s}\sum_{k=1}^{K_s} d^0_{s,h}(l,k). \tag{14}$$

In a similar way, one can approximate the expected hourly power loss in the system when no DSS is installed. Note, however, that computation of $c^y_{s,h}$ is not necessary for the optimal DSS placement problem as will be explained soon. Nonetheless, the relevant details are provided here for completeness. Using real data of loads and renewable generation, the expected hourly power loss at the planning year can be approximated as:

$$\begin{aligned} c^0_{s,h} &= \frac{1}{2}\mathbb{E}\left\{[\mathbf{d}^0_{s,h}]^T\, \mathbf{M}\, [\mathbf{d}^0_{s,h}]\right\} \\ &= \frac{1}{2}\sum_{l=1}^{2(N-1)}\sum_{r=1}^{2(N-1)} m_{l,r}\mathbb{E}\left\{d^0_{s,h}(l)d^0_{s,h}(r)\right\} \\ &\approx \frac{1}{2K_s}\sum_{l=1}^{2(N-1)}\sum_{r=1}^{2(N-1)}\sum_{k=1}^{K_s} m_{l,r}d^0_{s,h}(l,k)d^0_{s,h}(r,k) \end{aligned} \tag{15}$$

where $m_{l,r}$ is the (l,r) element of $\mathbf{M}$.

Computation of the above-mentioned expectations for the whole planning horizon requires the statistics of the vector of stochastic net demands in future years. This can be computed based on its current statistics as well as the anticipated growth rate of the load and renewable generations. Let the net demand data points at the planning time be decomposed as $d^0_{s,h}(l,k) = d^{0,\text{load}}_{s,h}(l,k) - d^{0,\text{DG}}_{s,h}(l,k)$, corresponding to the load and DGs. Assume a fixed annual growth rate of γ_{load} and γ_{DG} for the the load and renewable generation, respectively. Then $\bar{\mathbf{d}}^y_{s,h}$ and $c^y_{s,h}$ for $y \geq 1$ can be computed by (14) and (15), respectively, with $d^0_{s,h}(l,k)$ replaced by $d^y_{s,h}(l,k) = [\gamma_{\text{load}}]^y d^{0,\text{load}}_{s,h}(l,k) - [\gamma_{\text{DG}}]^y d^{0,\text{DG}}_{s,h}(l,k)$.

Finally, the expected economic gain of SGO due to the reduction in the active power loss in the yth year of the planning horizon is given by:

$$\Gamma^{\text{loss}}_y(\mathbf{\Pi}) = \frac{365}{\mathsf{S}}\sum_{s=1}^{\mathsf{S}}\sum_{h=1}^{24} \eta^y_{s,h}c^y_{s,h} - \mathbb{E}\left\{\sum_{h=1}^{24} \eta^y_{s,h}\mathrm{L}^y_{s,h}\left(\mathbf{d}^{\text{DSS}}_{s,h}\right)\right\}. \tag{16}$$

Observe from (16) and (12) that the terms corresponding to $c^y_{s,h}$ cancel out in Γ^{loss}_y. Therefore, Γ^{loss}_y contains only quadratic and linear terms of $\mathbf{\Pi}$. This is indeed expected as $\Gamma^{\text{loss}}_y(\mathbf{0})$ should be equal to zero. In other words, when no DSS is installed in the system, there will be no economic gain. Also note that the Hessian of $\Gamma^{\text{loss}}_y(\mathbf{\Pi})$ with respect to $\mathbf{\Pi}$ is equal to $\frac{-1}{\mathsf{S}} \times \text{diag}\{\eta^y_{1,1}\mathbf{M}, \eta^y_{2,1}\mathbf{M}, \ldots, \eta^y_{\mathsf{S},1}\mathbf{M}, \ldots, \eta^y_{\mathsf{S},24}\mathbf{M}\}$, which is negative semi-definite, because $\mathbf{M} \succeq 0$ and $\eta^y_{s,h} > 0, \forall h, \forall s, \forall y$. Therefore, $\Gamma^{\text{loss}}_y(\mathbf{\Pi})$ is concave in $\mathbf{\Pi}$.

C. The Reduction in Expected Price of Renewable Energy Curtailed

Due to the intermittent nature of renewable energy sources, there may be times when the technical system constraints are about to be violated due to excess distributed generation. Under such circumstances, the SGO may have to curtail the non-dispatchable renewable generations. However, if the system is equipped with DSS, they can be optimally operated to reduce the curtailment of renewable energy sources. This section addresses the economic gain of DSS installation in terms of reducing the non-dispatchable energy curtailment. The average economic gain due to lower energy curtailment in year y will be refered to as $\Gamma^{\text{curt}}_y(\mathbf{\Pi})$.

It is difficult to explicitly formulate the expected economic value of the spilled energy due to violation of system constraints. Instead, an indirect approach is taken in this paper. Here, we regularize the objective function of the DSS placement with a virtual term associated with the improvement in the voltage profile of the system. With this virtual benefit included in the objective function, the DSS placement routine will try to avoid the violation of system constraints. Once the storage units are optimally placed in the system and their operation strategy is optimized, the actual economic value of the spilled energy will be approximated through Monte Carlo simulations.

To regularize the objective function with regards to the voltage profile of the system, first note that in distribution systems the imaginary part of the voltages are very small (the voltage angles are very small). Therefore, one can approximate the magnitude of the nodal voltages by their real parts. As a result, the total expected deviation in the real parts of the nodal voltages, with respect to the flat voltage profile, can serve as an index for evaluation of the voltage profile. Now consider the decomposition $\mathbf{A} = [\mathbf{A}_\mathbf{e}^T \ \mathbf{A}_\mathbf{f}^T]^T$ for the matrix in (2), where $\mathbf{A_e}$ and $\mathbf{A_f}$ are $(N-1) \times 2(N-1)$ matrices corresponding to the real and imaginary parts, respectively. Let $\mathbf{e}^y_{s,h}(\mathbf{p}^{\text{DSS}}_{\mathbf{s,h}})$ be the vector of deviations in the real parts of the nodal voltages at hour h, segment s, and year y. Similarly to the way that the expected reduction in the power loss was computed in Section III-B, the average improvement in the voltage profile during the planning horizon due to installation of DSS can be formulated as:

$$\Gamma^{\text{vol}}(\mathbf{\Pi}) = \frac{365}{\mathsf{SY}} \sum_{s,y} \mathbb{E}\left\{ \sum_{h=1}^{24} \left\|\mathbf{e}^y_{s,h}(\mathbf{0})\right\|^2 - \left\|\mathbf{e}^y_{s,h}(\mathbf{d}^{\text{DSS}}_{s,h})\right\|^2 \right\}$$

$$= \frac{-1}{\mathsf{SY}} \sum_{s,y} \sum_{h=1}^{24} \left[\mathbf{d}^{\text{DSS}}_{s,h}\right]^T \mathbf{A}_\mathbf{e}^T \mathbf{A_e} \left[\mathbf{d}^{\text{DSS}}_{s,h}\right]$$

$$+ 2 \sum_{h \in \mathcal{H}_o} [\bar{\mathbf{d}}^y_{s,h}]^T \ \mathbf{A}_\mathbf{e}^T \mathbf{A_e} \left[\mathbf{d}^{\text{DSS}}_{s,h}\right]$$

$$- 2 \sum_{h \in \mathcal{H}_p} [\bar{\mathbf{d}}^y_{s,h}]^T \mathbf{A}_\mathbf{e}^T \mathbf{A_e} \left[\mathbf{d}^{\text{DSS}}_{s,h}\right]. \tag{17}$$

In (17), $\bar{\mathbf{d}}^y_{s,h}$ can be approximated using LLN as in (14). Observe that the Hessian of $\Gamma^{\text{vol}}(\mathbf{\Pi})$ with respect to $\mathbf{\Pi}$ is equal to $\frac{-2}{\mathsf{SY}} \times \text{diag}\{\mathbf{A}_\mathbf{e}^T\mathbf{A_e}, \mathbf{A}_\mathbf{e}^T\mathbf{A_e}, \ldots, \mathbf{A}_\mathbf{e}^T\mathbf{A_e}\}$ which is negative semi-definite, because $\mathbf{A}_\mathbf{e}^T\mathbf{A_e} \succeq 0$ by structure. Therefore, $\Gamma^{\text{vol}}(\mathbf{\Pi})$ is concave in the operation strategy of the DSS.

The limits on the amount of reverse power flow from distribution system to the sub-transmission system may also result in the curtailment of renewable energy sources [10]. Thus, the reverse power flow limits in the system may affect the planning of DSS [26]. If the reverse power limit at the substation is high enough, however, there is no need for DSS in terms of prevention of the non-dispatchable energy spillage [26]. For instance, the Ontario Power Authority allows for a 60% reverse power flow through the substation transformer [10]. This amount of reverse power limit will accommodate many scenarios of high generation of non-dispatchable DGs. Nonetheless, the installation of DSS can still be financially justifiable if other economic gains are noticeable. Depending on whether or not reverse active/reactive power flow is allowed in the system, the smart grid may also have different operating states [27], [28]. Similarly to [10], [27], and the references therein, the operating state considered in this paper only allows for the reverse active power flow to the sub-transmission system. We further assume that the reverse active power flow to the sub-transmission system is allowed without any rejection [29]. Note that the amount of excessive power in the system is random and will be known only at the operation stage. Nevertheless, at the planning stage which is the focus of this paper, one can require that the reverse reactive power constraint is respected on average. That is,

$$\mathbf{1}^T \left(\mathbb{E}\left\{\mathbf{q}_{s,h}\right\} - \mathbf{q}^{\text{DSS}}_{s,h}\right) \geq 0, \qquad \forall s, h, \tag{18}$$

where $\mathbb{E}\left\{\mathbf{q}_{s,h}\right\}$ is the average net reactive demand of the system.

Once the optimal DSS planning strategy is obtained for the system, the expected price of renewable energy curtailed will be computed for the system with and without DSS. Without loss of generality, assume that the wind turbines are candidates of energy curtailment as they are more likely to be utility-owned.[3] Using linearized power flow equations, the optimal curtailment strategy seeking the minimum power curtailment to satisfy the system constraints, can be formulated as:

$$\min \quad \mathbf{1}^T \mathbf{d}^{\text{curt}} \tag{19}$$

subject to.

$$\mathbf{0} \leq \mathbf{p}^{\text{curt}} \leq \mathbf{p}^{\text{wind}} \tag{20}$$

$$\mathbf{0} \leq \mathbf{q}^{\text{curt}} \leq \mathbf{q}^{\text{DSS}} \tag{21}$$

$$\mathbf{1}^T \left(\mathbf{q}_{s,h} - \mathbf{q}^{\text{DSS}}\right) \geq 0, \tag{22}$$

[3]The formulation presented in the paper can simply accommodate the curtailment of solar generation as well.

$$\mathbf{v}^{\min} \leq \mathbf{A_e}\left(\mathbf{d}+\mathbf{d}^{\text{curt}}\right) \leq \mathbf{v}^{\max} \tag{23}$$

$$|I_l(\mathbf{d}^{\text{curt}})|^2 \leq |I_l^{\max}|^2, \quad l=1,2,\ldots,L, \tag{24}$$

where $\mathbf{d}^{\text{curt}} = [(\mathbf{p}^{\text{curt}})^T, (\mathbf{q}^{\text{curt}})^T]^T$ is the vector of curtailed active and reactive powers and $\mathbf{p}^{\text{wind}}$ is the vector of power generations by wind turbines. Constraints (21)–(22) suggest that the reactive power injection of the DSS may need to be curtailed to respect the reverse reactive power constraint of the substation. However, this constraint is not likely to be active as the reverse reactive power constraint of the substation was taken into consideration in (18) during the planning stage. In (23), $\mathbf{v}^{\min}$ and $\mathbf{v}^{\max}$ are the vector of minimum and maximum allowable voltage limits, respectively. Also, $\mathbf{d}$ is the vector of forecast total demand of the nodes for the next hour. When DSS are installed in the system, the vector $\mathbf{d}$ also includes the optimized injection and consumption of the storage units. In (24), $|I_l|$ is the magnitude of the current flowing in branch l, $I_l^{\max}$ is the ampacity of branch l, and L is the total number of branches in the system. It is shown in Appendix B that the quadratic term (24) is convex in $\mathbf{d}^{\text{curt}}$. Therefore, (19) is a convex optimization problem. Note, however, that due to the inherent approximation of the linearized power flow equations, the solution of (19) is a rough estimate of the curtailed powers. To find an accurate solution, one can solve (19) for coarse tuning the curtailed powers and then do grid search along with ACPF to fine tune the results.

D. The Improvement in the System Resilience

In this section the economic value of the DSS in terms of improving the system resilience is formulated.

Let $\mathcal{H}_o(h) \in \mathcal{H}_o$ be the set of off-peak hours from the beginning of the off-peak period up to the hour h. Similarly, let $\mathcal{H}_p(h) \in \mathcal{H}_p$ be the set of peak hours from the beginning of the peak period up to the hour h. Also, let $0 < \beta_{ch} < 1$ and $0 < \beta_{dis} < 1$ be the charging and discharging efficiencies of the DSS technology used, respectively. Hence, $\beta_{rt} = \beta_{ch}\beta_{dis} < 1$ is the round-trip efficiency of the storage units. Denote the total energy that the DSS can supply to the grid in segment s and at the end of hour h by $\mathcal{E}_{s,h}(\mathbf{\Pi})$. Since $\mathcal{E}_{s,h}$ is equal to the total energy stored in the storage units times β_{dis}, one can write:

$$\mathcal{E}_{s,h} = \begin{cases} \beta_{rt} \sum_{h' \in \mathcal{H}_o(h)} \mathbf{1}^T \mathbf{p}_{s,h'}^{\text{DSS}}, & h \in \mathcal{H}_o \\ \beta_{rt} \sum_{h' \in \mathcal{H}_o} \mathbf{1}^T \mathbf{p}_{s,h'}^{\text{DSS}} - \sum_{h' \in \mathcal{H}_p(h)} \mathbf{1}^T \mathbf{p}_{s,h'}^{\text{DSS}}, & h \in \mathcal{H}_p \end{cases}$$

Upon imposing appropriate charging/discharging constraints, as will be done in Section IV, $\mathcal{E}_{s,h}$ is guaranteed to be nonnegative. In the event that the primary supply of the system is interrupted, the distribution system may be operated as an islanded microgrid. In such a case, the local DGs as well as the energy stored in the DSS can supply the loads of the system for a limited time. The non-critical loads of the system may need to be shed depending on the availability of the energy by local sources. Therefore, $\mathcal{E}_{s,h}$ can be viewed as the additional amount of load that can be preserved each time the supply from the primary source has failed. In distribution systems, the System Average Interruption Frequency Index (SAIFI) measures the average number of power interruptions a customer experiences during one year. Let $\bar{\mu}_y$ be the expected interruption cost per 1 kWh of energy in year y of the planning horizon. In practice, the interruption cost per unit kWh is a function of the interruption duration as well [30]. However, one can use the Customer Average Interruption Duration Index (CAIDI) to find an approximate value for the expected interruption cost. Let $\xi_{s,h}$ be the fraction of the interruptions that occur at hour h during segment s of each year, see [30]. The average economic value of the DSS in terms of enhancing the resilience of the system can be approximated as:

$$\Gamma_y^{\text{res}}(\mathbf{\Pi}) = \bar{\mu}_y \times \text{SAIFI} \times \sum_h \sum_s \xi_{s,h} \mathcal{E}_{s,h}. \tag{25}$$

Note that $\Gamma_y^{\text{res}}(\mathbf{\Pi})$ is linear in $\mathcal{E}_{s,h}$ and, hence, in $\mathbf{\Pi}$.

E. The Economic Gain of the System Upgrade Deferral

Due to the constant load growth in distribution systems, the system will require an upgrade in the feeder ampacities and substation capacity at some point in the future. However, if DSS are installed in the system, they can be employed to shave the load at peak hours and thereby defer the required upgrade of the system [4], [15].

In order to defer the upgrade of the system, the objective function of the DSS placement can include a term to shave the peak load in the system. To that end, form the expected total active power drawn from the substation during peak hours as:

$$P_{s,h}^{\text{peak}}(\mathbf{\Pi}) = \mathbb{E}\left\{\mathbf{1}^T(\mathbf{p}_{s,h}^{\mathbf{Y}} - \mathbf{p}_{s,h}^{\text{DSS}})\right\}, \quad \forall s,h \in \mathcal{H}_p, \tag{26}$$

where $\mathbf{1}$ and $\mathbf{0}$ are of size $(N-1)\times 1$. The optimization routine will try to lower the maximum of $P_h^{\text{peak}}(\mathbf{\Pi})$ over peak hours as will be explained in the next section. Note that the expected total active load in (26) has been computed for the last year of the planning horizon because the last year is supposed to have the maximum demand.

Once the DSS is optimally planned in the system, the economic gain of deferring the system upgrade due to installation of DSS will be computed. As per common practice of distribution system planning, the system constraints have to be satisfied for all combinations of the load and distributed generation. To evaluate the latest possible time for the system upgrade, the histograms of the available real data are examined to find the maximum values of the load and minimum values of the distributed generation based a predetermined confidence interval. Then, for each year of the planning horizon a power flow is run according to the the extreme loading and generation to find the required ampacity of the feeders and substations. Then, the upgrade requirements of the feeders and substation of the system are calculated for the system with and without DSS [15]. Finally, the average yearly difference in the system upgrade cost for the yth year, denoted by $\Gamma_y^{\text{up}}(\mathbf{\Pi})$, is computed.

IV. The Optimal Distributed Storage Planning Problem

This section aims at formulating the optimal DSS planning problem in smart distribution grids. To that end, the *regularized*

expected discounted gain of the SGO due to installation of DSS is defined as:

$$\Gamma'(\mathbf{\Pi}) = \omega_1 \Gamma^{\text{vol}}(\mathbf{\Pi}) - \omega_2 \Delta + \sum_{y=1}^{\mathsf{Y}} \lambda^y \left\{ \Gamma_y^{\text{arb}}(\mathbf{\Pi}) + \Gamma_y^{\text{loss}}(\mathbf{\Pi}) + \Gamma_y^{\text{res}}(\mathbf{\Pi}) \right\}, \quad (27)$$

where $\omega_1, \omega_2 > 0$ are two regularization factors and Δ is an auxiliary variable used for shaving the peak load as will be explained shortly (see (34)). Also, $0 < \lambda < 1$ is the discount factor. If the interest rate is int and a uniform inflation rate of inf is assumed for the energy price and the interruption cost, then $\lambda = (1 + \text{inf})/(1 + \text{int})$. The regularization parameters ω_1 and ω_2 will be tuned based on simulations to yield the best trade-off between the investment cost and the economic gain of the DSS. The tuning of the regularization parameters can be done using a grid search. Note that based on the formulations presented in Section III, $\Gamma'(\mathbf{\Pi})$ is concave in $\mathbf{\Pi}$.

In order to formulate the investment cost of the DSS, let $\mathbf{b} = [b_2, b_3, \ldots, b_N]^T$ be the capacity of the installed storage units in kWh. Also, let κ_1 \$/kWh be the unit cost of the DSS technology used and κ_2 \$/kVA be the associated power electronics and O&M costs. Then, the initial investment cost of DSS in the system is equal to $\kappa_1 1^T \mathbf{b} + \kappa_2 1^T \mathbf{r}$, where $\mathbf{r} = [r_2, r_3, \ldots, r_n]^T$ is the vector of rated powers of the storage units. Now, assume that the planning horizon is greater than the lifetime of the DSS with a factor of K, i.e., $\mathsf{Y} = \mathsf{K} \times \mathsf{Y}_{\text{DSS}}$, where Y_{DSS} is the DSS lifetime in years. Then, the storage units need to be replaced in the system K times. Therefore, the discounted investment cost of storage units will be given by:

$$\Omega(\mathbf{b}, \mathbf{r}) = \kappa_1' 1^T \mathbf{b} + \kappa_2 1^T \mathbf{r}, \quad (28)$$

where $\kappa_1' = \kappa_1 \times \sum_{\mathsf{k}=0}^{\mathsf{K}-1} \lambda^{\mathsf{k}\mathsf{Y}_{\text{DSS}}}$. Observe from (28) that $\Omega(\mathbf{b}, \mathbf{r})$ is linear in $\mathbf{b}$ and $\mathbf{r}$.

The optimal DSS planning aiming at maximizing the economic gain minus the investment cost can now be cast as the following optimization problem:

$$\max_{\mathbf{b}, \mathbf{r}, \mathbf{\Pi}} \Gamma'(\mathbf{\Pi}) - \Omega(\mathbf{b}, \mathbf{r}) \quad (29)$$

subject to a series of constraints as follows.

1) *The power capability of the storage units:* The active and reactive power injection of the DSS are jointly constrained by the power capability curve of the DSS [12], [25]. This can be modeled by the following quadratic, convex constraint:

$$\left(\mathbf{p}_{s,h}^{\text{DSS}}\right)^2 + \left(\mathbf{q}_{s,h}^{\text{DSS}}\right)^2 \leq \mathbf{r}^2, \quad \forall s, h. \quad (30)$$

Note that the notation is slightly abused in (30) as $(\cdot)^2$ is used to denote element-wise exponentiation of the vectors. In practice, one could use a set of arbitrarily accurate linearized constraints equivalent to (30) as done in [12]. Recall that to ensure a longer lifetime for the storage units, they are restricted to charge during off-peak hours and discharge during peak hours [10], [25]. Throughout Section III, the charging and discharging strategies of the active power of the DSS are differentiated by appropriate positive and negative signs. Therefore, the following constraint should be added to the optimal planning problem:

$$\mathbf{p}_{s,h}^{\text{DSS}} \geq \mathbf{0}, \quad \forall s, h. \quad (31)$$

2) *The charging/discharging capacity of the storage units:* Discharging the storage units completely affects their lifetime adversely [31]. In particular, the lifetime of the storage units is dependent on their maximum Depth Of Discharge (DOD) [17], [31]. Let γ_{DOD} be the maximum DOD of the storage units. The parameter γ_{DOD} along with β_{ch} and β_{dis} determines how much energy is needed to charge a storage unit of a given capacity during off-peak hours. The first time that a storage unit of size b_n is connected to node n, a total energy of $(1 - \gamma_{\text{DOD}})b_n$ kWh is absorbed which remains in the unit and never discharges. Next, an amount of up to $\gamma_{\text{DOD}} b_n$ kWh is absorbed from the grid during the next charging cycle. Therefore, for charging cycles (off-peak hours) one can write:

$$\beta_{ch} \sum_{h \in \mathcal{H}_o} \mathbf{p}_{s,h}^{\text{DSS}} = \gamma_{\text{DOD}} \mathbf{b}, \quad \forall s. \quad (32)$$

Similarly, at peak hours when the storage units get discharged, the total energy absorbed by the units during off-peak hours times the discharging efficiency will be equal to the total energy injected to the grid. That is,

$$\sum_{h \in \mathcal{H}_p} \mathbf{p}_{s,h}^{\text{DSS}} = \beta_{dis} \beta_{ch} \sum_{h \in \mathcal{H}_o} \mathbf{p}_{s,h}^{\text{DSS}}, \quad \forall s. \quad (33)$$

Since the values of the charging and discharging powers are assumed to be non-negative in our formulation, the constraints (32) and (33) require that the charging/discharging power of each node be zero if no storage unit is installed on the node.

3) *The maximum peak load:* The parameter Δ in (27) serves to represent the maximum peak load over peak hours. Hence, the following set of linear constraints has to be added to the optimal DSS placement problem:

$$P_{s,h}^{\text{peak}}(\mathbf{\Pi}) \leq \Delta, \quad \forall s, h \in \mathcal{H}_p \quad (34)$$

where $P_{s,h}^{\text{peak}}(\mathbf{\Pi})$ is defined in (26).

Once the optimal DSS planning problem (29) is solved, the total discounted economic gain of the SGO will be computed as:

$$\Gamma(\mathbf{\Pi}) = \sum_{y=1}^{\mathsf{Y}} \lambda^y \left\{ \Gamma_y^{\text{arb}}(\mathbf{\Pi}) + \Gamma_y^{\text{loss}}(\mathbf{\Pi}) + \Gamma_y^{\text{res}}(\mathbf{\Pi}) + \Gamma_y^{\text{curt}}(\mathbf{\Pi}) + \Gamma_y^{\text{up}}(\mathbf{\Pi}) \right\}. \quad (35)$$

Note that the explicit formulation of $\Gamma_y^{\text{curt}}(\mathbf{\Pi})$ and $\Gamma_y^{\text{up}}(\mathbf{\Pi})$ in terms of $\mathbf{\Pi}$ is intractable and, hence, the regularized expected discounted gain $\Gamma'(\mathbf{\Pi})$ is considered for optimal DSS planning instead of $\Gamma(\mathbf{\Pi})$.

V. Numerical Results

This section presents the numerical results of the optimal DSS planning methodology on a modified 69-node, 11 kV distribution system [24].

The simulations presented in the paper were done using MATPOWER [32] on a computer with 8 GB memory and a Core i5 CPU of frequency 2.7 GHz. The optimal DSS planning problem was solved using the branch and bound algorithm, which was implemented using the CVX package [33] bundled with Mosek [34].

A. The Setting of the Simulations

The modified test system is radial (all tie line switches are open) with four feeders where node 1 is considered as the slack node. The total nominal demand of the system in the first year of the planning period is $4468 + j3059$ kVA. The power factor of each node is derived from the nominal active and reactive demand of the node based on the information reported in [24]. For this system, inclined solar cells are considered on 34 randomly selected nodes of the grid. The nodes equipped with solar cells are 3, 4, 6, 8, 10, 13, 17, 19, 20, 22, 23, 30, 31, 32, 33, 35, 36, 37, 40, 44, 45, 46, 49, 51, 53, 55, 57, 58, 61, 62, 63, 65, 67, 68. A total rated power of 1000 kW is considered for the solar cells in this test system. This total rated power is allocated to the solar cell-equipped nodes proportionally to their secondary transformer power rating. In addition, two wind turbines are installed on the nodes 21 and 50 with power ratings of 400 kW and 800 kW, respectively. The reverse power flow is allowed for the active power only without any rejection.

In our simulations, the Advanced Metering Infrastructure (AMI) data released by the Commission for Energy Regulation (CER) [35] is utilized to model the loads. The dataset provided by CER is from the Electricity Customer Behaviour Trail study and has been collected from 5000 smart meters in Ireland from July 14, 2009 to December 31, 2010. This dataset was received by authors from Irish Social Science Data Archive (ISSDA) [36]. The reactive power demands are modeled by assuming a constant power factor for the nodes. A growth of 5% [17] in the demands of the nodes is considered over the planning horizon. The time series of wind generation and solar generation are obtained from [37] and [38], respectively.

The DSS technology used is lead-acid with specifications provided in [39]. The DSS are assumed to come in 100 kVA–100 kWh units with charging and discharging efficiency of $\beta_{ch} = \beta_{dis} = 0.85$. In order to guarantee that the lifetime of the storage units is not shortened, the DOD of the storage units is assumed to be $\gamma_{\text{DOD}} = 0.75$ [31]. The minimum and maximum voltage limits for all nodes are considered to be 0.95 p.u. and 1.05 p.u., respectively. The DSS costs are 305 \$/kWh for the storage units and replacements, 175 \$/kVA for the inverter, and 15 \$/kVA for annual maintenance. The planning horizon is assumed to be twice as the lifetime of the DSS and each year is divided into 12 segments.

The price of energy is considered to be 8.29 ¢/kWh for off-peak hours and 12.43 ¢/kWh for peak hours. The interest rate and the inflation rates are assumed 5% and 1%, respectively. Also, μ is considered 15 \$/kWh based on the survey reported in [30] and SAIFI is 1.5.

The system upgrade includes upgrading the distribution system feeders and substation. In addition, similarly to [4], it is assumed that a 25 km transmission line between the distribution substation and the HV/MV primary substation needs to be upgraded too. The upgrade costs of lines, feeders and substations are obtained from [40].

B. Results

The optimal DSS planning methodology on the system under study results in the installation of one storage unit of size 200 kWh with an inverter power rating of 100 kVA. The optimal location of this unit is node 29 which is on feeder 2. Note that the optimization routine was not enforced to place only one storage unit in the system. In other words, the optimal DSS planning could have conceivably resulted in the placement of more than one unit, possibly on different nodes of the system. The placement of only one storage unit, its location, its power rating and capacity, and its charging and discharging strategy are rather the optimal setting to yield the maximum expected discounted reward. Fig. 1 illustrates the test system under study with the optimal location of the storage unit. The locations of the two wind turbines are also shown in Fig. 1. In this figure, the nodes equipped with solar cells are indicated with shadow.

Fig. 2 depicts the optimal State Of Charge (SOC) of the installed storage unit for three different segments of the year. It is apparent from Fig. 2 that the optimal SOC of the storage unit is different for different segments of the year. This is because the statistics of the loads and renewable energy sources change over different hours of the day and different segments of the year. Accordingly, the optimal charging and discharging strategy of the storage unit is different for different hours and segments. To see how the statistics of the load and renewable energy sources impact the optimal charging and discharging strategy of the storage unit, the expected total net demand of the first year of the system is also depicted in Fig. 3. Here, the total expected ned demand refers to the arithmetic average of the total load minus total renewable generation in the system among all the days belonging to the segment. It can be seen from Figs. 2 and 3 that the optimized strategy makes the storage unit charge when the expected total net demand is low (off-peak hours) and discharge when the expected total net demand is high (peak hours.) Inspection of Figs. 2 and 3 reveals that the sharp peak of the Segment 5 causes the storage unit to discharge quickly over just two hours, while a smoother peak of the Segment 11 results in a smoother discharge over 6 hours. In contrast to Segment 11 which has a smooth off-peak demand, in Segments 5 and 8, the demand at $h \approx 1$ is very higher than the minimum demand which happens at $h \approx 5$. As a result, the storage unit does not charge at $h = 1$ for Segments 5 and 8, and starts charging only at $h = 2$. During mid hours when the demand is not very high or very low, the storage unit neither absorbs nor injects any power in any of the segments.

The total investment cost for this storage unit will be \$141,310, which includes the following:

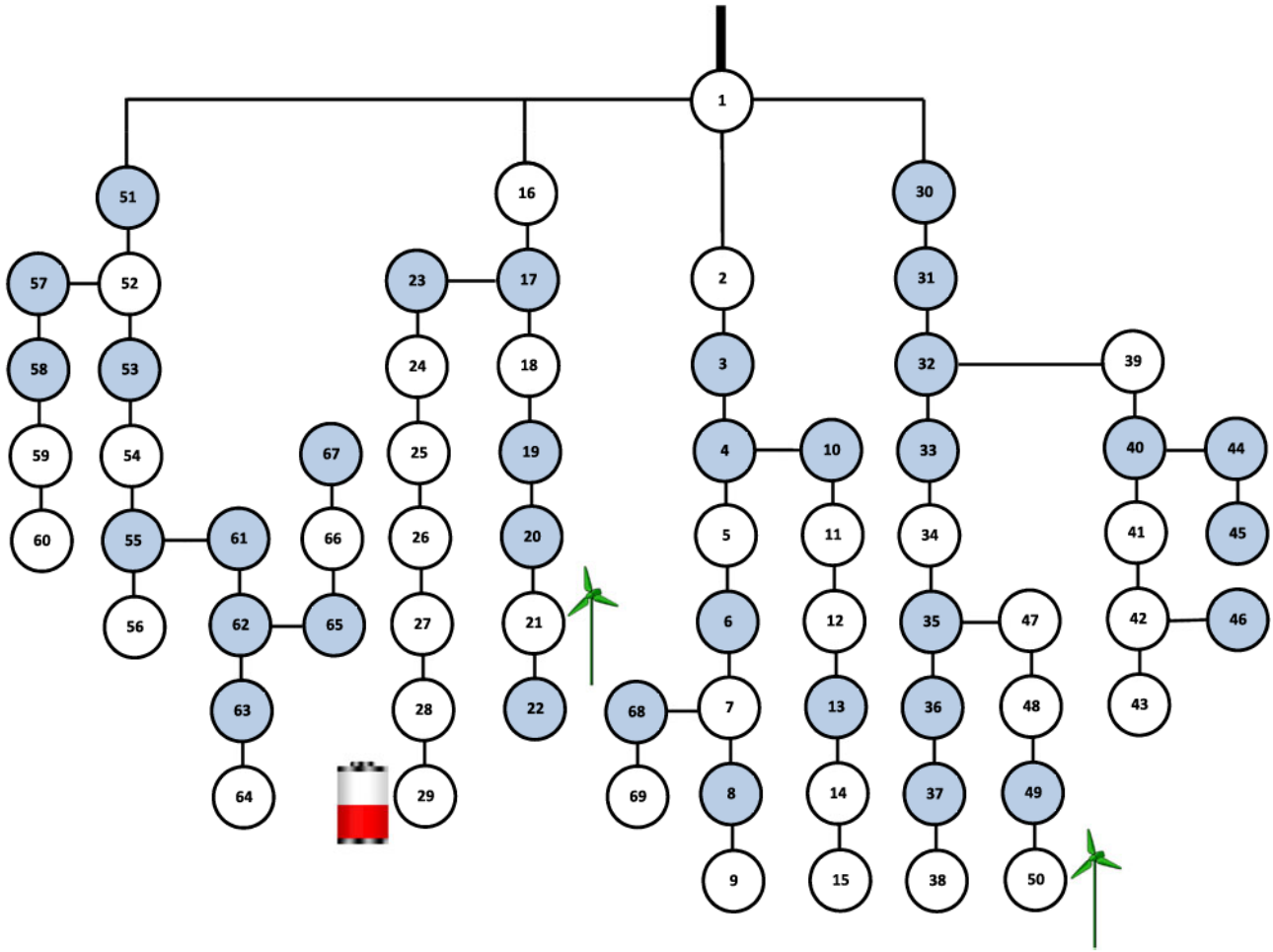

Fig. 1. The test system under study with wind turbines and solar cells and the storage unit optimally located on node 29.

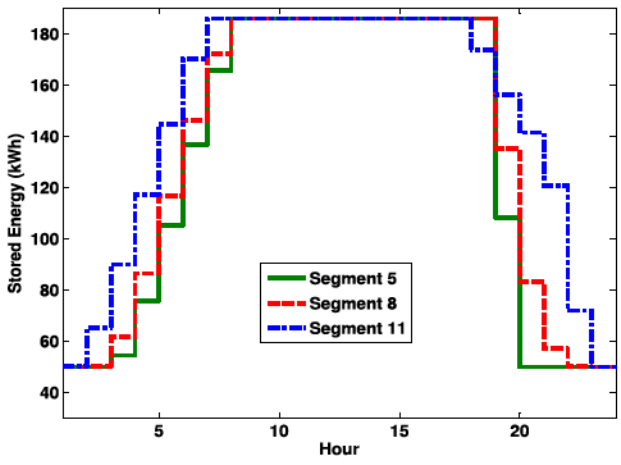

Fig. 2. The optimal SOC of the installed storage unit for three different segments of the year.

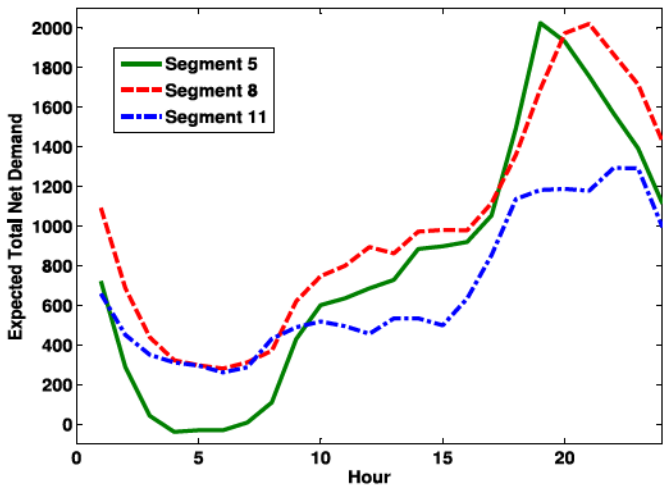

Fig. 3. The expected total net demand of the system for three different segments of the first year.

1) Initial investment cost: $78,500
2) Replacement cost: $43,006
3) Total discounted maintenance cost: $19,804

With the optimal DSS placement in the system, the SGO is expected to obtain the following gains during the entire planning horizon:

1) Expected discounted arbitrage gain: $6,135
2) Expected discounted gain due to reduction in the system losses: $8,181
3) Expected discounted economic value of system resilience enhancement: $24,854

4) Expected discounted gain due to reduction in the renewable energy curtailment: \$235
5) Total economic gain due to deferring the upgrade of the system: \$176,038

The upgrade time of the system is determined by running the Newton's AC power flow for the future years and under the following two cases: the maximum load along with minimum renewable generation and the minimum load along with maximum renewable generation. The minimum and maximum values of the loads and renewable generation are obtained by examining the available real data set. If some system equipment need to be upgraded, the required increase in their capacity is evaluated. Based on our simulations, the feeders of the test system will need to be upgraded in a year. Feeder 2, in particular, will be upgraded to accommodate an additional 1.5 MW. According to the upgrade costs reported in [40], this requires a total investment of \$336,000. Based on our simulations, the installation of DSS can postpone this task for another two years. Therefore, considering the discount factor $\lambda = 1.01/1.05 = 0.9619$, a financial gain of $(\lambda - \lambda^3) \times 336,000 = \$24,159$ is achievable. In addition, the existing capacity of the substation of the system is 4.5 MW. With a 5% annual increase in the demands, the system should accommodate 10.83 MW at the end of the planning horizon. Therefore, an additional capacity of 6.33 MW will be needed. According to the upgrade costs reported in [40], this would require an investment of \$516,500. Based on our simulations, the optimal planning of DSS can postpone the upgrade cost of the substation by one year, resulting in a financial gain of $(1 - \lambda) \times 516,500 = \$19,679$. Finally, the transmission line between the distribution substation and the HV/MV primary substation needs to be upgraded in two years. According to [40], this would require an investment cost of \$3,750,000. With the help of DSS, this investment can be postponed from two years to three years, which would result in a financial gain of $(\lambda^2 - \lambda^3) \times 3,750,000 = \$132,200$. Therefore, the total saving in the upgrade costs would be $19,679 + 24,159 + 132,200 = \$176,038$.

Based on the above-mentioned numbers, the total discounted gain that the SGO obtains due to installation of DSS will be \$215,443. Given that the total investment and maintenance cost of DSS installation is \$141,310, we conclude that energy storage in this system results in a total discounted saving of \$74,133.

C. Computational Cost and Scalability

In terms of the computational cost of the optimization, the bottleneck is the number of integer variables. Since the storage units are assumed to have integer capacity and integer power rating, the number of integer variables in the proposed methodology is $2N$. However, the computational cost can be reduced if, similarly to some existing literature [14]–[16], only some candidate nodes are considered for DSS installation rather than all the nodes. Moreover, the computational time can be significantly reduced if, instead of a zero duality gap, a very small duality gap (e.g., 0.5%) is considered satisfactory. Table I demonstrates this fact by showing the impact of the number of candidate nodes and the desired duality gap on the computational time of the optimization. It can be seen from Table I that the computational time of the solution obtained for a 0.5% duality gap is significantly smaller than that of the the zero duality gap. More importantly, the computational time of the solution obtained for a 0.5% duality gap scales much better in the number of candidate nodes compared with the solution obtained for a zero duality gap.

TABLE I
IMPACT OF THE NUMBER OF CANDIDATE NODES AND THE DUALITY GAP ON THE COMPUTATIONAL TIME OF THE OPTIMIZATION

Number of Candidate Nodes	CPU Time (s) (Duality gap = 0)	CPU Time (s) (Duality gap < 0.5%)
9	5.3	1.9
17	17.6	3.9
34	101.0	10.2
69	1571.6	28.7

We finish this section by noting that increasing the number of segments per year can potentially lead to a better DSS planning with a better cost-benefit trade-off. On the other hand, increasing the number of segments will increase the size and the computational costs of the optimization problem. The authors will explore this aspect of the problem in their future research.

VI. CONCLUSION

This paper presented a methodology for optimal planning of DSS in smart distribution grids. The problem of optimizing the expected economic gain of the system operator was formulated as a mixed-integer convex program. In particular, the optimal planning problem incorporated the arbitrage gain, the reduction in the active power loss, the reduction in the non-dispatchable energy curtailment, the improvement in the system resilience, and the financial gain due to deferring the system upgrade to future years. The stochasticity of the loads and renewable energy sources was treated in a statistically rigorous way by evaluating the mathematical expectations using the Law of Large Numbers. Numerical results using real data of smart meters and renewable sources on a typical distribution system was presented which demonstrated the effectiveness of using DSS in future smart grids.

APPENDIX A

In this Appendix we derive the quadratic form of (7) for the active power loss of the distribution systems using the results presented in [41] and show that the loss function is convex in the demand vector.

For ease of notation define the augmented vectors $\hat{\mathbf{e}} = [0 \;\; \mathbf{e}^T]^T$, $\hat{\mathbf{f}} = [0 \;\; \mathbf{f}^T]^T$, and $\hat{\mathbf{p}} = [p_{\text{slack}}, p_2 - p_{\text{DG},2}, p_3 - p_{\text{DG},3}, \ldots, p_N - p_{\text{DG},N}]$. Also, let $\hat{\mathbf{i}}$ be the vector of current injections to the system. If the voltage of the slack node is 1 p.u., the active power loss in the system can be written as [41]:

$$\begin{aligned} L &= \mathbf{1}^T \hat{\mathbf{p}} \\ &= \Re\{(\mathbf{1} + \hat{\mathbf{e}} + j\hat{\mathbf{f}})^T \hat{\mathbf{i}}^*\} \\ &= \Re\{(\mathbf{1} + \hat{\mathbf{e}} + j\hat{\mathbf{f}})^T [\mathbf{Y}(\mathbf{1} + \hat{\mathbf{e}} + j\hat{\mathbf{f}})]^*\} \end{aligned}$$

$$= \Re\{(\hat{\mathbf{e}} + j\hat{\mathbf{f}})^T \mathbf{Y}^*(\hat{\mathbf{e}} - j\hat{\mathbf{f}})\} \tag{36}$$

$$= \Re\{(\hat{\mathbf{e}} + j\hat{\mathbf{f}})^T (\mathbf{G} - j\mathbf{B})(\hat{\mathbf{e}} - j\hat{\mathbf{f}})\}$$

$$= \hat{\mathbf{e}}^T \mathbf{G}\hat{\mathbf{e}} + \hat{\mathbf{f}}^T \mathbf{G}\hat{\mathbf{f}}$$

$$= \mathbf{e}^T \tilde{\mathbf{G}}\mathbf{e} + \mathbf{f}^T \tilde{\mathbf{G}}\mathbf{f}, \tag{37}$$

where (36) follows from the fact that $\mathbf{Y}^*\mathbf{1} = \mathbf{0}$ and $\mathbf{1}^T\mathbf{Y}^* = \mathbf{0}$. Equation (37) can also be written in a matrix form as:

$$L(\mathbf{e};\mathbf{f}) = \begin{bmatrix} \mathbf{e} \\ \mathbf{f} \end{bmatrix}^T \begin{bmatrix} \tilde{\mathbf{G}} & \mathbf{0} \\ \mathbf{0} & \tilde{\mathbf{G}} \end{bmatrix} \begin{bmatrix} \mathbf{e} \\ \mathbf{f} \end{bmatrix}. \tag{38}$$

Equation (7) then follows by substituting the the linearized power flow equations (6) into (38).

To establish the convexity of the loss function $L(\mathbf{d})$ in the demand vector $\mathbf{d}$, we need to show that $\nabla^2 L(\mathbf{d}) = \mathbf{M} \succeq 0$. To that end, first note that the system admittance matrix is positive semi-definite, that is $\mathbf{G} \succeq 0$. In [41], this is shown using the fact that the active power loss in the system is non-negative for all values of the nodal voltages. Next, note that for a positive semi-definite matrix, all the principal submatrices have to be positive semi-definite. Therefore, it follows from the positive semi-definiteness of $\mathbf{G}$ that $\tilde{\mathbf{G}}$ is positive semi-definite, too. As a result, for any x and y belonging to $\mathbb{R}^{N-1}$, we have:

$$\begin{bmatrix} x \\ y \end{bmatrix}^T \begin{bmatrix} \tilde{\mathbf{G}} & \mathbf{0} \\ \mathbf{0} & \tilde{\mathbf{G}} \end{bmatrix} \begin{bmatrix} x \\ y \end{bmatrix} = x^T \tilde{\mathbf{G}} x + y^T \tilde{\mathbf{G}} y \geq 0. \tag{39}$$

Because $\tilde{\mathbf{G}}$ is also symmetric and real, the following Cholesky decomposition exists:

$$\begin{bmatrix} \tilde{\mathbf{G}} & \mathbf{0} \\ \mathbf{0} & \tilde{\mathbf{G}} \end{bmatrix} = \mathbf{U}\mathbf{U}^T, \tag{40}$$

where $\mathbf{U}$ is a real, lower triangular matrix with positive diagonal entries. Therefore, for any $\mathbf{z} \in \mathbb{R}^{N-1}$, we have:

$$\mathbf{z}^T \mathbf{M}\mathbf{z} = 2\mathbf{z}^T \mathbf{A}^T \mathbf{U}\mathbf{U}^T \mathbf{A}\mathbf{z}$$

$$= 2(\mathbf{U}^T \mathbf{A}\mathbf{z})^T (\mathbf{U}^T \mathbf{A}\mathbf{z})$$

$$= 2\|\mathbf{U}^T \mathbf{A}\mathbf{z}\|_2^2 \geq 0, \tag{41}$$

which demonstrates that $\mathbf{M}$ is positive semi-definite.

APPENDIX B

In this appendix we show that the quadratic form of (24) is convex in $\mathbf{d}^{\text{curt}}$.

Let $i = i_{\text{re}} + j i_{\text{im}}$ be the vector of currents in the branches of the system. Also, let $\mathbf{Y}_{\text{br}}$ be the branch admittance matrix of the system. Then the vector of branch currents corresponding to the total demand of $\mathbf{d} + \mathbf{d}^{\text{curt}}$ is given by:

$$I = \mathbf{Y}_{\text{br}}(\mathbf{1} + \hat{\mathbf{e}} + j\hat{\mathbf{f}})$$

$$= \mathbf{Y}_{\text{br}}(\hat{\mathbf{e}} + j\hat{\mathbf{f}}) \tag{42}$$

$$= \tilde{\mathbf{Y}}_{\text{br}}(\mathbf{e} + j\mathbf{f})$$

$$= (\tilde{\mathbf{G}}_{\text{br}}\mathbf{e} - \tilde{\mathbf{B}}_{\text{br}}\mathbf{f}) + j(\tilde{\mathbf{G}}_{\text{br}}\mathbf{f} + \tilde{\mathbf{B}}_{\text{br}}\mathbf{e})$$

$$= \left[(\tilde{\mathbf{G}}_{\text{br}}\mathbf{A}_{\mathbf{e}} - \tilde{\mathbf{B}}_{\text{br}}\mathbf{A}_{\mathbf{f}}) + j(\tilde{\mathbf{G}}_{\text{br}}\mathbf{A}_{\mathbf{f}} + \tilde{\mathbf{B}}_{\text{br}}\mathbf{A}_{\mathbf{e}})\right](\mathbf{d} + \mathbf{d}^{\text{curt}})$$

$$= \mathbf{T}^{\text{re}}(\mathbf{d} + \mathbf{d}^{\text{curt}}) + j\mathbf{T}^{\text{im}}(\mathbf{d} + \mathbf{d}^{\text{curt}}), \tag{43}$$

where $\mathbf{T}^{\text{re}} = \tilde{\mathbf{G}}_{\text{br}}\mathbf{A}_{\mathbf{e}} - \tilde{\mathbf{B}}_{\text{br}}\mathbf{A}_{\mathbf{f}}$, $\mathbf{T}^{\text{im}} = \tilde{\mathbf{G}}_{\text{br}}\mathbf{A}_{\mathbf{f}} + \tilde{\mathbf{B}}_{\text{br}}\mathbf{A}_{\mathbf{e}}$. Also, $\tilde{\mathbf{Y}}_{\text{br}} = \tilde{\mathbf{G}}_{\text{br}} + j\tilde{\mathbf{B}}_{\text{br}}$ is the branch admittance matrix with the first column removed. Moreover, (42) stems from the fact that $\mathbf{Y}_{\text{br}}\mathbf{1} = \mathbf{0}$. Let $\mathbf{t}_{\text{re},l}^T$ and $\mathbf{t}_{\text{im},l}^T$ be the lth row of $\mathbf{T}^{\text{re}}$ and $\mathbf{T}^{\text{im}}$, respectively. Then, the magnitude of the currents in the branches of the system as a function of the curtailment vector $\mathbf{d}^{\text{curt}}$ will be given by:

$$|I_l(\mathbf{d}^{\text{curt}})|^2 = \left(\mathbf{t}_{\text{re},l}^T(\mathbf{d} + \mathbf{d}^{\text{curt}})\right)^2 + \left(\mathbf{t}_{\text{im},l}^T(\mathbf{d} + \mathbf{d}^{\text{curt}})\right)^2$$

$$= (\mathbf{d} + \mathbf{d}^{\text{curt}})^T \mathbf{t}_{\text{re},l}\mathbf{t}_{\text{re},l}^T(\mathbf{d} + \mathbf{d}^{\text{curt}})$$

$$+ (\mathbf{d} + \mathbf{d}^{\text{curt}})^T \mathbf{t}_{\text{im},l}\mathbf{t}_{\text{im},l}^T(\mathbf{d} + \mathbf{d}^{\text{curt}})$$

$$= (\mathbf{d} + \mathbf{d}^{\text{curt}})^T \mathbf{T}_l(\mathbf{d} + \mathbf{d}^{\text{curt}}), \tag{44}$$

where $\mathbf{T}_l = \mathbf{t}_{\text{re},l}\mathbf{t}_{\text{re},l}^T + \mathbf{t}_{\text{im},l}\mathbf{t}_{\text{im},l}^T$. Now observe that the matrices $\mathbf{t}_{\text{re},l}\mathbf{t}_{\text{re},l}^T$ and $\mathbf{t}_{\text{im},l}\mathbf{t}_{\text{im},l}^T$ are positive semi-definite by structure. Therefore, $\mathbf{T}_l$ is positive semi-definite, too.

REFERENCES

[1] A. Gabash and P. Li, "Flexible optimal operation of battery storage systems for energy supply networks," *IEEE Trans. Power Syst.*, vol. 28, no. 3, pp. 2788–2797, Aug. 2013.

[2] C. P. Nguyen and A. J. Flueck, "Agent based restoration with distributed energy storage support in smart grids," *IEEE Trans. Smart Grid*, vol. 3, no. 2, pp. 1029–1038, Jun. 2012.

[3] T. Jiang, Y. Cao, L. Yu, and Z. Wang, "Load shaping strategy based on energy storage and dynamic pricing in smart grid," *IEEE Trans. Smart Grid*, vol. 5, no. 6, pp. 2868–2876, Nov. 2014.

[4] A. Oudalov, D. Chartouni, C. Ohler, and G. Linhofer, "Value analysis of battery energy storage applications in power systems," in *Proc. Power Syst. Conf. Expo.*, 2006, pp. 2206–2211.

[5] K. Christakou, D.-C. Tomozei, M. Bahramipanah, J.-Y. Le Boudec, and M. Paolone, "Primary voltage control in active distribution networks via broadcast signals: The case of distributed storage," *IEEE Trans. Smart Grid*, vol. 5, no. 5, pp. 2314–2325, Sep. 2014.

[6] P. Wang, D. H. Liang, J. Yi, P. F. Lyons, P. J. Davison, and P. C. Taylor, "Integrating electrical energy storage into coordinated voltage control schemes for distribution networks," *IEEE Trans. Smart Grid*, vol. 5, no. 2, pp. 1018–1032, Mar. 2014.

[7] B. P. Roberts and C. Sandberg, "The role of energy storage in development of smart grids," *Proc. IEEE*, vol. 99, no. 6, pp. 1139–1144, Jun. 2011.

[8] A. Nagarajan and R. Ayyanar, "Design and strategy for the deployment of energy storage systems in a distribution feeder with penetration of renewable resources," *IEEE Trans. Sustain. Energy*, vol. 6, no. 3, pp. 1085–1092, Jul. 2015.

[9] Q. Li, R. Ayyanar, and V. Vittal, "Convex optimization for DES planning and operation in radial distribution systems with high penetration of photovoltaic resources," *IEEE Trans. Sustain. Energy*, vol. 7, no. 3, pp. 985–995, Jul. 2016.

[10] Y. M. Atwa and E. El-Saadany, "Optimal allocation of ESS in distribution systems with a high penetration of wind energy," *IEEE Trans. Power Syst.*, vol. 25, no. 4, pp. 1815–1822, Nov. 2010.

[11] J. Tant, F. Geth, D. Six, P. Tant, and J. Driesen, "Multiobjective battery storage to improve PV integration in residential distribution grids," *IEEE Trans. Sustain. Energy*, vol. 4, no. 1, pp. 182–191, Jan. 2013.

[12] M. Nick, R. Cherkaoui, and M. Paolone, "Optimal allocation of dispersed energy storage systems in active distribution networks for energy balance and grid support," *IEEE Trans. Power Syst.*, vol. 29, no. 5, pp. 2300–2310, Sep. 2014.

[13] A. S. Awad *et al.*,"Optimal ESS allocation and load shedding for improving distribution system reliability," *IEEE Trans. Smart Grid*, vol. 5, no. 5, pp. 2339–2349, Sep. 2014.
[14] M. Sedghi, A. Ahmadian, and M. Aliakbar-Golkar, "Optimal storage planning in active distribution network considering uncertainty of wind power distributed generation," *IEEE Trans. Power Syst.*, vol. 31, no. 1, pp. 304–316, Jan. 2016.
[15] A. S. Awad, T. H. El-Fouly, and M. Salama, "Optimal ESS allocation for load management application," *IEEE Trans. Power Syst.*, vol. 30, no. 1, pp. 327–336, Jan. 2015.
[16] A. S. Awad, T. H. EL-Fouly, and M. Salama, "Optimal ESS allocation for benefit maximization in distribution networks," *IEEE Trans.* vol. 8, no. 4, pp. 1668–1678, Jul. 2017.
[17] G. Carpinelli, G. Celli, S. Mocci, F. Mottola, F. Pilo, and D. Proto, "Optimal integration of distributed energy storage devices in smart grids," *IEEE Trans. Smart Grid*, vol. 4, no. 2, pp. 985–995, Jan. 2013.
[18] P. Xiong and C. Singh, "Optimal planning of storage in power systems integrated with wind power generation," *IEEE Trans. Sustain. Energy*, vol. 7, no. 1, pp. 232–240, Jan. 2016.
[19] S. Hashemi, J. Ostergaard, and G. Yang, "A scenario-based approach for energy storage capacity determination in LV grids with high PV penetration," *IEEE Trans. Smart Grid*, vol. 5, no. 3, pp. 1514–1522, May 2014.
[20] S. Bolognani and S. Zampieri, "On the existence and linear approximation of the power flow solution in power distribution networks," *IEEE Trans. Power Syst.*, vol. 31, no. 1, pp. 163–172, Jan. 2016.
[21] R. Baldick, "DC power flow in rectangular coordinates," in *Proc. DIMACS Workshop Energy Infrastruct., Des. Stability Resilience*, Feb. 2013.
[22] S. V. Dhople, S. S. Guggilam, and Y. C. Chen, "Linear approximations to AC power flow in rectangular coordinates," *IEEE Communicat., Control, Comput. (Allerton), 53rd Annual Allerton Conf.*, pp. 211–217, 2015.
[23] M. Ghasemi Damavandi, V. Krishnamurthy, and J. R. Martí, "Robust meter placement for state estimation in active distribution systems," *IEEE Trans. Smart Grid*, vol. 6, no. 4, pp. 1972–1982, Jul. 2015.
[24] D. Das, "A fuzzy multiobjective approach for network reconfiguration of distribution systems," *IEEE Trans. Power Del.*, vol. 21, no. 1, pp. 202–209, Jan. 2006.
[25] A. Gabash and P. Li, "Active-reactive optimal power flow in distribution networks with embedded generation and battery storage," *IEEE Trans. Power Syst.*, vol. 27, no. 4, pp. 2026–2035, Nov. 2012.
[26] A. Gabash, M. Alkal, and P. Li, "Impact of allowed reverse active power flow on planning PVs and BSSs in distribution networks considering demand and EVs growth," in *Proc. IEEE Power Energy Student Summit*, Bielefeld, Germany, 2013, pp. 23–25.
[27] A. Gabash and P. Li, "On variable reverse power flow—Part I: Active-Reactive optimal power flow with reactive power of wind stations," *Energies*, vol. 9, no. 3, p. 121, 2016.
[28] A. Gabash and P. Li, "On variable reverse power flow—Part II: An electricity market model considering wind station size and location," *Energies*, vol. 9, no. 4, p. 235, 2016.
[29] A. Gabash, D. Xie, and P. Li, "Analysis of influence factors on rejected active power from active distribution networks," in *Proc. IEEE Power Energy Student Summit*, 2012, pp. 25–29.
[30] M. Sullivan, J. Schellenberg, and M. Blundell, "Updated value of service reliability estimates for electric utility customers in the United States," Ernest Orlando Lawrence Berkeley Nat. Lab., Berkeley, CA, USA, Tech. Rep., 2015.
[31] K. Divya and J. Østergaard, "Battery energy storage technology for power systems-An overview," *Elect. Power Syst. Res.*, vol. 79, no. 4, pp. 511–520, 2009.
[32] R. D. Zimmerman, "MATPOWER: A MATLAB power system simulation package."
[33] M. Grant, S. Boyd, and Y. Ye, "CVX: MATLAB software for disciplined convex programming," 2008.
[34] MOSEK ApS, "The MOSEK optimization toolbox for MATLAB manual. Version 7.1 (Revision 28)," 2015. [Online]. Available: http://docs.mosek.com/7.1/toolbox/index.html
[35] Commission for Energy Regulation (CER). Customer Behaviour Trials (CBTs). [Online]. Available: http://www.cer.ie/electricity-gas/smart-metering/
[36] Irish Social Science Data Archive. CER Smart Metering Project. [Online]. Available: http://www.ucd.ie/issda/data/commissionforenergyregulationcer/
[37] EirGrid. [Online]. Available: http://www.eirgrid.com/operations/systemperformancedata/
[38] Solar Radiation Data. [Online]. Available: http://www.soda-is.com/eng/services/
[39] P. Poonpun and W. T. Jewell, "Analysis of the cost per kilowatt hour to store electricity," *IEEE Trans. Energy Convers.*, vol. 23, no. 2, pp. 529–534, Jun. 2008.
[40] S. Wong, K. Bhattacharya, and J. D. Fuller, "Electric power distribution system design and planning in a deregulated environment," *IET Gener., Transm. Distrib.*, vol. 3, no. 12, pp. 1061–1078, 2009.
[41] S. De la Torre and F. D. Galiana, "On the convexity of the system loss function," *IEEE Trans. Power Syst.*, vol. 20, no. 4, pp. 2061–2069, Nov. 2005.

Authors' photographs and biographies not available at the time of publication.